

Article

The β -Fructofuranosidase from *Rhodotorula dairenensis*: Molecular Cloning, Heterologous Expression, and Evaluation of Its Transferase Activity

María Gimeno-Pérez, Zoran Merdzo , Eva Castillo-Rosa , Carlos Martín de Hijas 
and María Fernández-Lobato * 

Center of Molecular Biology Severo Ochoa (CSIC-UAM), Nicolás Cabrera 1. Universidad Autónoma de Madrid, 28049 Madrid, Spain; mgimeno@cbm.csic.es (M.G.-P.); zoran@cbm.csic.es (Z.M.); ecastillo@cbm.csic.es (E.C.-R.); carlos.mj93@gmail.com (C.M.d.H.)

* Correspondence: mfernandez@cbm.csic.es; Tel.: +34-91-1964492

Abstract: The β -fructofuranosidase from the yeast *Rhodotorula dairenensis* (RdINV) produces a mixture of potential prebiotic fructooligosaccharides (FOS) of the levan-, inulin- and neo-FOS series by transfructosylation of sucrose. In this work, the gene responsible for this activity was characterized and its functionality proved in *Pichia pastoris*. The amino acid sequence of the new protein contained most of the characteristic elements of β -fructofuranosidases included in the family 32 of the glycosyl hydrolases (GH32). The heterologous yeast produced a protein of about 170 kDa, where N-linked and O-linked carbohydrates constituted about 15% and 38% of the total protein mass, respectively. Biochemical and kinetic properties of the heterologous protein were similar to the native enzyme, including its ability to produce prebiotic sugars. The maximum concentration of FOS obtained was 82.2 g/L, of which 6-kestose represented about 59% (w/w) of the total products synthesized. The potential of RdINV to fructosylate 19 hydroxylated compounds was also explored, of which eight sugars and four alditols were modified. The flexibility to recognize diverse fructosyl acceptors makes this protein valuable to produce novel glycosyl-compounds with potential applications in food and pharmaceutical industries.

Keywords: *Rhodotorula*; fructooligosaccharides; *Pichia pastoris* expression system; family GH32; fructosylated compounds



Citation: Gimeno-Pérez, M.; Merdzo, Z.; Castillo-Rosa, E.; Hijas, C.M.d.; Fernández-Lobato, M. The β -Fructofuranosidase from *Rhodotorula dairenensis*: Molecular Cloning, Heterologous Expression, and Evaluation of Its Transferase Activity. *Catalysts* **2021**, *11*, 476. <https://doi.org/10.3390/catal11040476>

Academic Editors: Richard Daniellou and Zheng Guo

Received: 8 March 2021

Accepted: 4 April 2021

Published: 7 April 2021

Publisher's Note: MDPI stays neutral with regard to jurisdictional claims in published maps and institutional affiliations.



Copyright: © 2021 by the authors. Licensee MDPI, Basel, Switzerland. This article is an open access article distributed under the terms and conditions of the Creative Commons Attribution (CC BY) license (<https://creativecommons.org/licenses/by/4.0/>).

1. Introduction

The β -fructofuranosidases (EC 3.2.1.26) catalyze the release of fructose from the non-reducing termini of different-size fructans and sucrose (invertases). As well as hydrolysing sucrose, β -fructofuranosidases may also catalyze the synthesis of short-chain fructooligosaccharides (FOS), in which one to three fructosyl moieties are linked to a sucrose unit. Different FOS series can be distinguished depending on the linkage type between the monosaccharide residues: ¹F-FOS, containing β -(2-1)-linked fructose units (inulin-type structure, e.g., 1-kestose); ⁶F-FOS, containing β -(2-6)-linked fructose units (levan-type structure, e.g., 6-kestose); and ⁶G-FOS, where a β -(2-6) linkage connects fructose to the glucosyl moiety of sucrose (neo-FOS, e.g., neokestose). FOS selectively stimulate the growth and activity of health-promoting microbial species in the gut, the so-called prebiotic effect [1,2], stimulating or improving the immune and cardiovascular systems, mineral absorption, and even mental health [3–7]. Although the three series of FOS show beneficial effects, β -(2-6)-linked FOS appear to have improved prebiotic properties and increased chemical stability compared to the traditionally commercialized β -(2-1)-linked FOS [8,9]. In addition, neo-FOS also showed a potential inhibitory activity against melanoma cells and colon cancer [10,11].

Enzymatic synthesis of FOS has been reported using different microbial systems. Among others, β -fructofuranosidases from *Aspergillus* (main industrial producers) provide a mixture of sugars included in the 1 F-FOS series, whereas those from yeasts *Saccharomyces cerevisiae* and *Schwanniomyces occidentalis* produce mainly 6-kestose and, from *Xanthophyllomyces dendrorhous*, neokestose [12–17]. Although structural determinants responsible for the selective production of FOS by these proteins are not yet clear, the relevance of particular residues in substrate binding and product specificity has been demonstrated by mutational analyses [18–21]. The ability to produce FOS of β -fructofuranosidases from some species of the genus *Rhodotorula* has also been analyzed with different results. Curiously, enzymes from *Rhodotorula* sp.-LEB-V10 and *Rhodotorula mucilaginosa* only generated sugars included in the 1 F-FOS series, whereas that from *Rhodotorula glutinis*, a yeast synthesizing numerous valuable compounds (carotenoids and lipids among others) with a wide industrial usage, did not produce any type of FOS [22–25]. However, the large protein RdINV from *Rhodotorula dairenensis* (~170 kDa, of which N-linked carbohydrates constituted ~16% of the total mass) produced mainly 6-kestose, but also a varied mixture of FOS of the three referenced series [26], which makes it of biotechnological interest.

Based on structural features, β -fructofuranosidases are classified into the family 32 of the glycosyl hydrolases (GH32) (CAZy; <http://www.cazy.org>, accessed on 29 March 2021), which contains a characteristic five-blade β -propeller N-terminal module, in which the β -sheets are arranged around a central pocket that accommodates the active site [27,28]. Three conserved sequences, each containing a key acidic residue implicated in substrate binding and hydrolysis, are located in the protein active site: WMNDPNG (D acting as nucleophile), FRDP (D acting as stabilizer of transient state) and ECP (E acting as acid-base catalyst) [29]. Proteins of GH32 include an additional C-terminal β -sandwich domain implicated in their oligomerization and substrate recognition [18–20]. In this context, and although several genomes from yeasts included in the genus *Rhodotorula* have been sequenced [30–32], functionality of none of the DNA sequences a priori codifying for proteins included in the family GH32 was proven.

In this work, the gene responsible for the β -fructofuranosidase RdINV has been characterized, its functionality proven in *Pichia pastoris*, the biochemical properties of the heterologous protein analyzed, and its ability to fructosylate sucrose and a variety of hydroxylated compounds evaluated.

2. Results

2.1. Molecular Characterization of the Gene RdINV and Analysis of the Amino Acid Sequence Encoded

To isolate the gene encoding the β -fructofuranosidase from *R. dairenensis*, the enzyme was purified as referenced [26]. As expected, only a protein of ~170 kDa was detected by SDS-PAGE, which was initially processed for amino acid sequencing using tryptic and chymotryptic digestion followed by MALDI-TOF-MS analyses. Protein retrieved the three tryptic peptides: PQVHYSPPK (526.8 m/z), PAASSSWGAEENPFFTDK (906.4 m/z), and NPVLSVGSNQFR (659.4 m/z) (Table S1) that already aligned with part of the sequences of β -fructofuranosidases from fungi as *Cordyceps militaris* (ATY66193), *Aureobasidium melanogenum* (ARG411451), and *Papiliotrema aurea* (AFO84001), all included in the structural family GH32. In addition, this protein generated 14 chymotryptic peptides, three of them sharing part of their sequences with the referenced tryptic peptides (Table S1). By using primers directed to the peptide sequences characterized here (Table S2), a yeast genomic DNA sequence of 2559-bp was characterized, which included an open reading frame (ORF) of 2297-bp (potential gene *RdINV*) preceded by 129-bp. Two possible introns of 70 and 199-bp, flanked with the conserved sequence of yeast splicing sites, were also identified in the first half of the ORF and eliminated using specific primers.

The gene characterized here encoded a polypeptide of 675 amino acids with a predicted molecular mass of 70.8 kDa, an isoelectric point of 4.5 units, a possible signal peptide for protein secretion of 20 amino acids, and 16 potential N-glycosylation sites. The probability of the protein O-glycosylation was also high considering that 72% and 62% of serine and

threonine residues, respectively, could be glycosylated. All sequences found in the 170 kDa protein by MALDI-TOF-MS analyses (Table S1) were located in the encoded polypeptide. The overall deduced sequence of the potential protein RdINV was remarkably similar to proteins included in the family GH32, which had previously been functionally and structurally characterized. Furthermore, it was more similar to enzyme sequences from the ascomycete yeasts *S. cerevisiae* (40% identity and 73% coverage) and *Sch. occidentalis* (39% identity and 74% coverage), as well as *Aspergillus awamori* (34% identity and 78% coverage) than to those from the basidiomycetes *X. dendrorhous* (28% identity and 27% coverage) and *Aspergillus kawachii* (29% identity and 29% coverage).

Figure 1 shows a structural alignment of the catalytic domains of RdINV and some structurally resolved proteins from eukaryotic microorganisms. All conserved motifs of the family GH32 were recognized in the RdINV sequence. Among them, the consensus sequences: WMNDPNG (FMNDPNG in RdINV), FRDP, and MWECPDF (AYECPNL in RdINV), including the catalytic triad (in bold), were identified as Asp188 (nucleophile), Asp312 (stabilizer of the transition state), and Glu362 (acid base catalyst in the hydrolysis mechanisms), respectively. A structural model of this protein based on the homologous exo-inulinase from *A. awamori* AaEI [33], which showed the highest sequence coverage with RdINV, was obtained (Figure S1). This model displayed the characteristic bimodular architecture of the family GH32, a catalytic β -propeller, and β -sandwich domains linked by a short segment.

2.2. Functionality of the Gene RdINV and Heterologous Protein Size Analyses

The DNA sequence characterized from *R. dairenensis*, containing or not the two intronic sequences (constructions RdINV-pIB4 and cRdINV-pIB4, respectively), was included in *Pichia pastoris*. Yeast transformants were cultivated in BMG medium and the protein expression induced with methanol as referenced [34]. The β -fructofuranosidase activity was only detected in transformants carrying construction cRdINV-pIB4. Figure 2 shows data obtained with one of the selected clones. Both activity levels and expression of an extracellular protein of ~170 kDa increased, as did the induction time. Maxima levels of activity (~25 U/mL; ~55 μ g/mL) were detected in yeast culture filtrates after 96 h of methanol induction. As expected, no activity was detected in transformants, including the empty plasmid pIB4, providing a direct evidence that gene *RdINV* truly directs the synthesis of the β -fructofuranosidase activity.

The β -fructofuranosidase purified from *R. dairenensis* and *P. pastoris* showed apparently the same molecular mass, ~170 kDa (Figure 3a), which is far from the theoretical ~70 kDa calculated on the basis of the protein RdINV deduced sequence. Treatment of the heterologous protein with PNGase F led a band of ~144 kDa, which implied that ~15.3% of the protein mass was due to N-glycosylation (Figure 3b). Similar results were previously obtained with the enzyme expressed in *R. dairenensis* [26]. No change in the electrophoretic mobility of the protein was obtained after using a mixture of O-glycosidase and neuroaminidase (data not shown), but the treatment with α -(1-2,3,6) mannosidase resulted in two bands of ~105 and ~80 kDa (Figure 3b, lanes 6–8). The sequential digestion with PNGase F first and then with mannosidase produced the same two-band pattern (Figure 3c). All these data pointed to glycosylation constituting almost 53% of the total protein molecular mass.

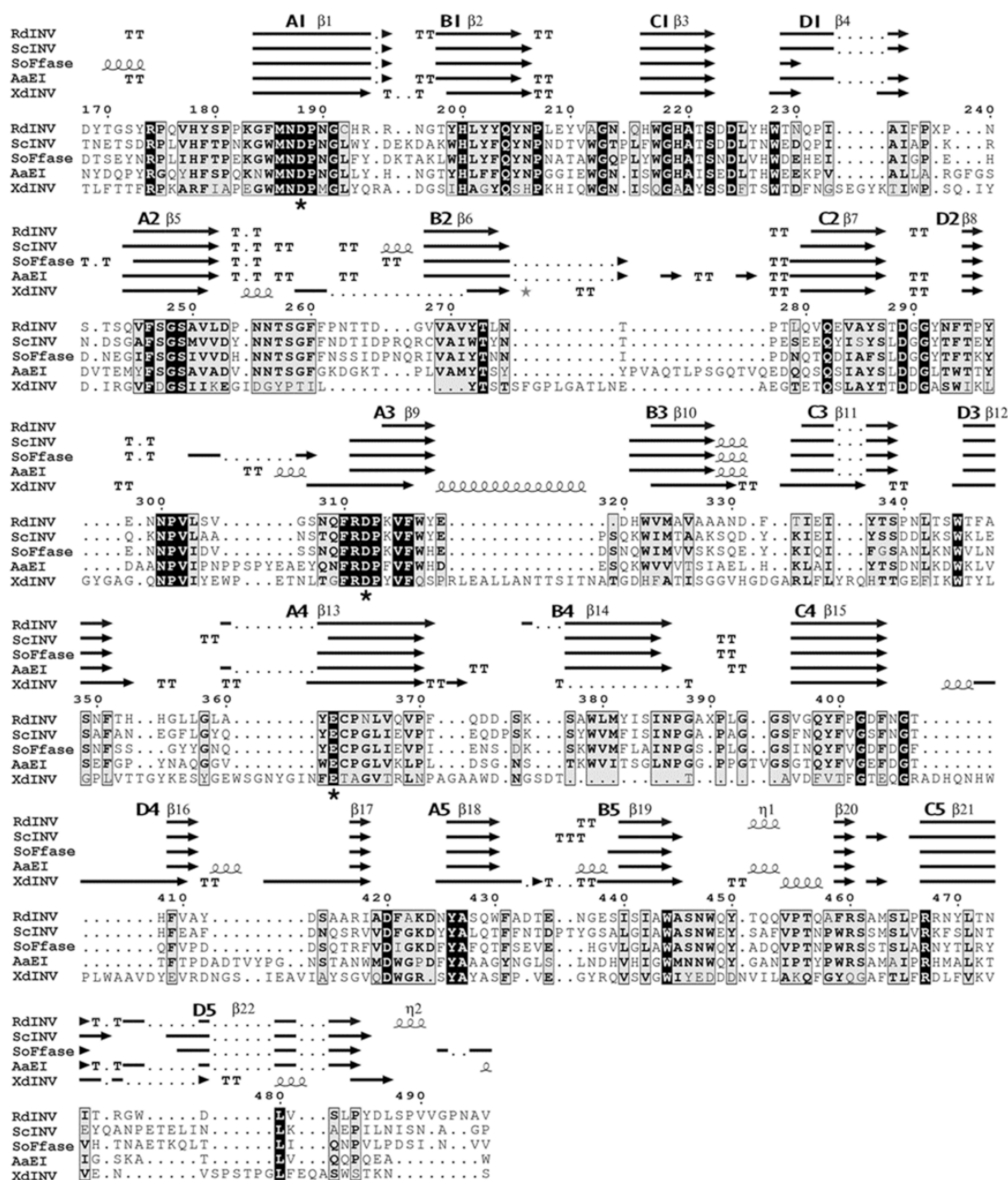


Figure 1. Structural alignment of family 32 of the glycosyl hydrolases (GH32) catalytic domain from yeasts and fungi. Predicted catalytic domain of RdINV (178–496 residues) was superimposed to the *S. cerevisiae* invertase (ScINV, PDB code 4EQV), *Sch. occidentalis* β -fructofuranosidase (SoFfase, PDB code 3KF5), *A. awamori* exoinulinase (AaEI, PDB code 1YM9) and *X. dendrorhous* β -fructofuranosidase (XdINV, PDB code 5ANN) using ENDscript server. The black squares indicate amino acid similarity as calculated by MSAProbs. Secondary structure elements suggested by DSSP program are shown as squiggles for α -helix, arrows labeled β for β -strands, and strict α - and β -turns depicted by TTT and TT letters, respectively. β -Strands (A–D) of each blade (1–5) of the β -propeller were depicted. Catalytic residues are highlighted with black asterisks.

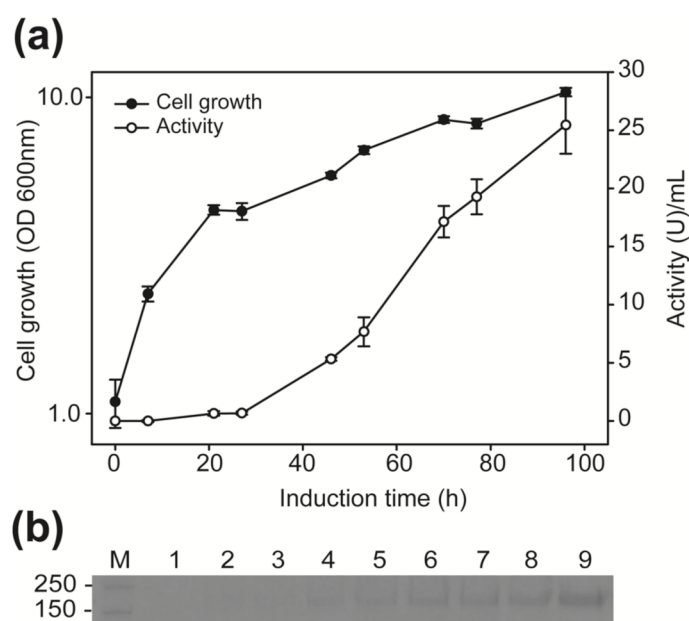


Figure 2. Time course of the β -fructofuranosidase produced in *P. pastoris*, including construction cRdINV-pIB4. **(a)** Yeast was cultured in 1-L flasks containing 200 mL of BMM (full circles), and extracellular activity (empty circles) was analyzed at the indicated times using sucrose as substrate. Each point represents the average of three independent measurements, and standard error are indicated. **(b)** Analysis on SDS-PAGE of the ~ 170 kDa protein detected at the times culture above was analyzed (lanes 1–9: 0, 7, 21, 27, 46, 53, 70, 77 and 96 h, respectively). Numbers on the left indicate the positions of molecular mass standards (lane M) in kDa.

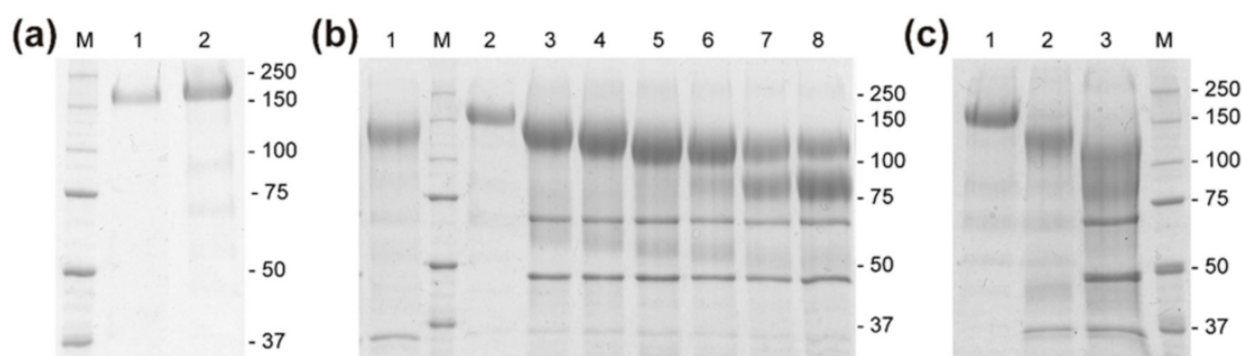


Figure 3. SDS-PAGE analysis of the purified β -fructofuranosidase RdINV and the deglycosylation treatment. **(a)** RdINV expressed in *R. dairenensis* (lane 1) and *P. pastoris* (lane 2). **(b)** The purified heterologous protein (lane 2) was treated with PNGase F (500 U) for 2 h (lane 1) or with mannosidase (2 U) during 1, 3, 8, 20, 48, and 72 h (lanes 3–8, respectively). **(c)** The heterologous protein (lane 1) was treated with PNGase F for 2 h (lane 2) and then with mannosidase for 7 h (lane 3). The positions of the molecular mass markers are indicated on the right in kDa. The theoretical molecular weight of PNGase F is 36 kDa and that of mannosidase 110 kDa, with two subunits of 66 and 44 kDa.

2.3. Analysis of the β -Fructofuranosidase Activity Expressed in *P. pastoris*

Biochemical characteristics of the β -fructofuranosidase RdINV expressed in the heterologous system were compared with those shown by the protein obtained from *R. dairenensis*. Proteins were purified and their activities at different pH and temperature values determined using sucrose as substrate. As previously published, the enzyme produced by *R. dairenensis* displayed maximum activity at pH 5.0 and 60 °C, retaining $\sim 35\%$ of activity at 70 °C [26]. In contrast, the heterologous protein showed it at pH 5.0 and 65 °C, retaining $\sim 50\%$ of activity at 80 °C (data not shown). The hydrolytic activity was also evaluated using

different sized substrates (Table 1). Regardless of the producing yeast (*R. dairenensis* or *P. pastoris*), the enzyme hydrolysed sucrose, raffinose, 1-kestose, inulin, and nystose, but not substrates such as melibiose, lactose, and lactulose. Additionally, it showed very similar K_m values for sucrose and 1-kestose, but the catalytic efficiency was two times higher for the one expressed in *R. dairenensis* compared to the heterologous enzyme (Table 2).

Table 1. Substrate specificity of RdINV expressed in the indicated yeast.

Substrate	β -Fructofuranosidase (U/mL)	
	<i>P. pastoris</i>	<i>R. dairenensis</i>
Sucrose	20.5 \pm 1.4	12.4 \pm 1.1
1-Kestose	4.1 \pm 0.03	1.8 \pm 0.02
Nystose	0.4 \pm 0.04	0.4 \pm 0.02
Raffinose	16.7 \pm 0.2	11.0 \pm 0.3
Inulin	3.2 \pm 0.05	2.8 \pm 0.03

Values are the average of three measures \pm standard errors.

Table 2. Kinetic parameters of RdINV expressed in the indicated yeast.

	Substrate	K_m (mM)	k_{cat} (1/s)	k_{cat}/K_m (1/s mM)
<i>P. pastoris</i>	Sucrose	6.2 \pm 1.0	2236 \pm 356	360 \pm 57
	1-Kestose	56 \pm 5	613 \pm 49	11 \pm 1
<i>R. dairenensis</i>	Sucrose	6.4 \pm 0.9	4458 \pm 628	698 \pm 98
	1-Kestose	57 \pm 4	1753 \pm 136	30 \pm 2

The transfructosylating activity of the protein expressed in *P. pastoris* was evaluated using sucrose as substrate. As expected, different FOS were detected in the reaction mixture, 6-kestose being the major transfructosylation product. Additionally, neokestose and 1-kestose, as well as the tetrasaccharides neonystose and nystose and the disaccharide blastose, were produced (Figure 4a). Similar chromatographic profiles were previously obtained with the enzyme expressed in *R. dairenensis*, but some of the products could not be identified because the corresponding standards were not available. In that case, ~68 and 11 g/L of 6-kestose and neokestose, respectively, were produced with a sucrose conversion close to 75% (w/w). The maximum concentration of FOS obtained in this work with the heterologous enzyme was 82.2 g/L (of which 6-kestose: 48.4 g/L; blastose and neokestose: 13.9 g/L each; neonystose: 3.1 g/L; 1-kestose: 2.9 g/L), representing ~14% (w/w) of the total carbohydrates in the reaction mixture, and was reached in 9 h, with a total sucrose conversion close to 80% (Figure 4b). A blastose increase concomitant with the decrease of neokestose was obtained after 11 h reaction, where neokestose reached 10.9 g/L (~22% reduction), neonystose 3 g/L, and blastose 15.9 g/L (~14% increase). At this point, 41.7 g/L of 6-kestose (~14% reduction) and 1.3 g/L of nystose were quantified. Maximum production of 6-kestose, 53.2 g/L, was reached after 7 h and represented ~59% (w/w) of the total FOS produced (Figure 4c). At that point, 12.2 g/L, 9.5 g/L, 2 g/L, and 1.9 g/L of neokestose, blastose, 1-kestose, and neonystose, respectively, were obtained.

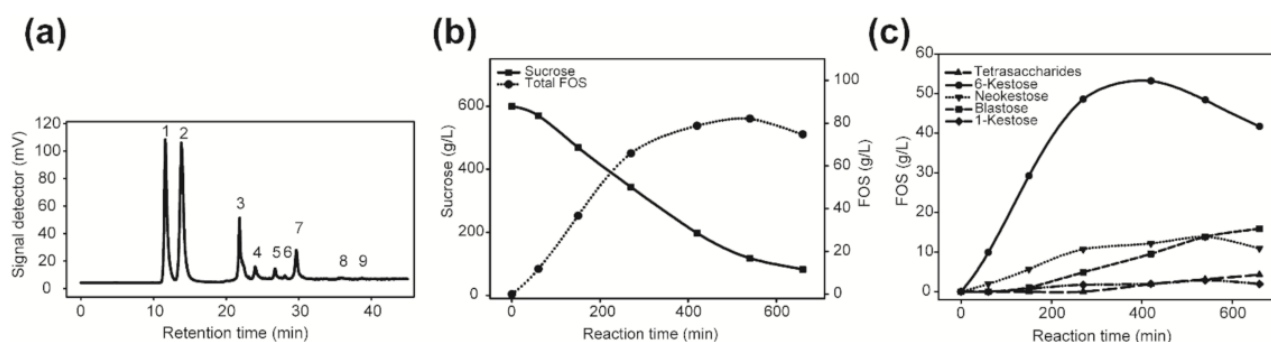


Figure 4. Transfructosylating reaction analysis catalyzed by RdINV. (a) HPLC chromatogram of the mixture obtained after 11 h reaction. Reaction conditions: 600 g/L sucrose at 60 °C. Peaks correspondence: (1) fructose, (2) glucose, (3) sucrose, (4) blastose, (5) neokestose, (6) 1-kestose, (7) 6-kestose, (8) neonystose, and (9) nystose. (b) Total fructooligosaccharides (FOS) production vs. the hydrolyzed sucrose. (c) Evolution of the different FOS detected in the reaction.

Reaction rate measurements were performed in triplicate. Values of k_{cat} were calculated considering a protein molecular mass of 170 kDa. The k_{cat}/K_m standard errors were obtained by fitting the normalized Michaelis–Menten equation $v = (k_{cat}/K_m) + [S]/(1 + [S]/K_m)$.

Potential of RdINV to synthesize new fructosylated products was explored using different hydroxylated acceptors alternative to sucrose in the transfructosylating reactions (Table 3). Chromatographic analyses of the reactions showed that two of the six monosaccharides assayed, glucose and fructose, significantly increased the blastose signal or generated two new peaks, respectively, which would be compatible with their fructosylation. Furthermore, six of the seven disaccharides and four of the six alditols assayed generated new peaks, which were absent in control reactions. Figure S2 shows some representative chromatograms of reactions including positive acceptors.

Table 3. Fructosyl-acceptor specificity of the RdINV expressed in *P. pastoris*.

Monosaccharides		Disaccharides		Polyols	
Acceptor	New Product ^a	Acceptor	New Product ^a	Acceptor	New Product ^a
Fructose	+	Trehalose	+	Erythritol	+
Galactose	-	Palatinose	+	Galactitol	+
Glucose	+	Lactose	+	Sorbitol	+
Xylose	-	Lactulose	+	Mannitol	+
Arabinose	-	Leucrose	+	Ribitol	-
Mannose	-	Maltose	+	Xylitol	-
		Melibiose	-		

^a +, transfructosylation for the new acceptor positive indicates that new peaks were detected in HPLC chromatograms.

3. Discussion

The β -fructofuranosidase RdINV from *R. dairenensis* produces sugars of 1F , 6F , and 6G -FOS series simultaneously, a property not shared by other β -fructofuranosidases from *Rhodotorula* spp. This fact, together with the large size of the N-deglycosylated protein, ~144 kDa, led us to address its molecular characterization. The gene *RdINV* characterized here was responsible for the analyzed β -fructofuranosidase activity since the encoded amino acid sequence already contained all the peptides detected in the protein purified from *R. dairenensis* and showed the consensus sequences of enzymes with proved fructosyl transferases activity. Indeed, enzymes containing the typical MNDPNG and ECP sequences have been classified as low-level FOS-synthesis enzymes, with FOS productions representing $\leq 20\%$ of total sugars in the reaction mixtures [29], and RdINV could be included in this group. In addition, potential proteins showing high similarity to RdINV were also

found in the genome of *Rhodotorula* sp. JG-1b (97% identity, 82% coverage; KWU45911) and *Rhodotorula graminis* (57% identity, 76% coverage; XP_018268095). RdINV showed a large N-terminal extension (177 amino acids) not present in other β -fructofuranosidases from yeasts but also showing similarity to other putative GH32 proteins from *Rhodotorula*, such as *Rhodotorula toruloides* (68.1% identity, 83% coverage; M7X5U7) and *Rhodotorula taiwanensis* (70.5% identity, 70% coverage; A0A2S5B6I2).

Functionality of the gene *RdINV* was analyzed in *P. pastoris*, basically, because this yeast lacks β -fructofuranosidase activity, shows high secretion of heterologous proteins, and a priori can process gene introns from other eukaryotic organisms [34]. However, protein RdINV, including a potential signal peptide of 20 amino acids, was only secreted by transformants containing the characterized gene without introns, which produced about 25 U/mL of β -fructofuranosidase activity (Figure 2a), thus, improving the level of activity reached by *R. dairenensis* cultures (1.9 U/mL) by about 13 times and reducing the protein purification process to a simple concentration step of a yeast extracellular medium.

The high molecular mass of RdINV (~170 kDa) was clearly due to its high degree of glycosylation since, after treatment with α -(1-2,3,6) mannosidase, it dropped to ~80 kDa, which is a similar size to other fungi deglycosylated β -fructofuranosidases [16,35,36]. The protein glycosylation profile is species-specific and important for the protein folding, which often is related to levels of protein secretion, stability, and/or activity [37,38]. Changes in the glycosylation pattern may lead to increased activity and/or stability when expressed in *P. pastoris* [38,39]. Accordingly, a different glycosylation pattern could also be responsible for variations of activity detected between enzymes produced in *R. dairenensis* and *P. pastoris* with the substrates tested in this work (Table 2), although the percentage of glycosylation was very similar in both cases (Figure 3).

The transferase activity of RdINV was not substantially altered after the expression in *P. pastoris*, as the main FOS produced was 6-kestose, followed by neokestose, 1-kestose, and two tetrasaccharides (Figure 4) that could be identified as neonystose and nystose. Blastose was also detected in reactions, a disaccharide previously obtained as a secondary product when using sucrose and the mycelium-bound transfructosylating activity of fungi, such as *Cladosporium cladosporioides* [40], and levansucrases from bacteria, such as *Zymomonas mobilis* [41]. It was also produced by β -fructofuranosidases from the yeast *Sch. occidentalis* and *X. dendrorhous* by direct fructosylation of glucose and hydrolysis of neokestose, respectively [34,42]. Curiously, RdINV could produce blastose using both ways since its production increased in reactions supplemented with glucose (Table 3, Figure S2a) and based exclusively on sucrose when the amount of neokestose was reduced (Figure 4c), which would make RdINV the first yeast enzyme showing this ability. In addition, RdINV was capable to transfer the fructosyl moiety of sucrose to a new unit of fructose, forming two products (Table 3 and Figure S2a). Most likely, in one of them, the two fructose units should be linked by a β -(2-6) bond due to the preference of RdINV to form 6-kestose, a levan-type trisaccharide where fructose units are connected by this linkage. The possibility of using *P. pastoris* cells to remove glucose [43] and fructose from the reaction mixtures is a very attractive possibility in order to obtain suitable FOS mixtures for diabetic patients, which we also intend to evaluate in the future. Moreover, some of the evaluated disaccharides were also fructosylated (Table 3): among them, palatinose and trehalose, which shared this characteristic with the β -fructofuranosidase from *X. dendrorhous*, but not with that from *Sch. occidentalis* [44,45]. RdINV also used different alditols as fructosylation acceptors, including erythritol and mannitol, which could improve their functional properties. These low-digestible molecules are considered a food supplement for people with diabetes and intestinal disorders, but they also could increase the bifidobacteria community in the human gut microbiome [46,47]. Therefore, the broad acceptor promiscuity of RdINV would increase its biotechnological potential and make it interesting for food and pharmacological sectors. Structural research of RdINV will help to understand the specificity and particular activity of this enzyme and provide more information to enlighten

the molecular mechanisms of the determinants responsible for fructosyltransferase activity, with the subsequent possibility to synthesize new oligosaccharides in a regioselective way.

4. Materials and Methods

4.1. Organisms, Growth and Expression Media

R. dairenensis CECT 1416 (also *R. glutinis* var. *dairenensis*) was cultured in MMM (0.7% yeast nitrogen base w/o amino acids [YNB], 2% maltose; all w/v) or YEP (1% yeast extract, 1% peptone, 2% glucose; all w/v) media. *P. pastoris* GS115 (his4; Invitrogen, Carlsbad, CA, USA) was used as expression host and was initially cultured in YEP. Yeast transformants carrying constructions based on plasmid pIB4 were selected on MD (1.34% YNB, 4×10^{-5} % biotin, 2% glucose), and protein expression was analyzed in BMM after growing in BMG (both media same as MD but in 100 mM potassium phosphate pH 6.0 and 0.5% methanol or 1% glycerol as carbon source, respectively), as reported previously [34]. Yeasts were cultivated at 28–30 °C and growth monitored spectrophotometrically at 600 nm (OD_{600}). *Escherichia coli* DH5 α was used for DNA manipulations using standard techniques.

4.2. Protein Purification, Quantification and Spectrometric Analysis

R. dairenensis was cultivated to stationary phase in MMM (1 L) and extracellular β -fructofuranosidase RdINV was purified as described [26]. In brief, yeast was grown for ~60 h (~4 ODU_{600} ; ~1.9 U/mL), culture filtrate was concentrated through 50000 MWCO PES and applied to a DEAE-Sephacel column equilibrated with 20 mM Tris-HCl pH 7. Samples eluting at 0.15 M salt were pooled and concentrated using Amicon Ultra-15 ultracel-100K filters to ~41 U/mL (~146 U/mg). A single band corresponding to an apparently pure protein of ~170 kDa was obtained by ProtoBlue Safe Colloidal Coomassie staining (National Scientific, Atlanta, GA, USA)-SDS-PAGE (8%). Precision Plus Protein Standards Unstained 10–250 kDa (Bio-Rad, Hercules, CA, USA) were used as markers. Protein concentration was determined by using Nano Drop-1000 Spectrophotometer (Thermo Fisher Scientific, Wilmington, DE, USA) at 280 nm.

For spectrometric analysis, proteins (~2 μ g) were excised from SDS-PAGE gels, digested in situ with trypsin or chymotrypsin and analyzed by Reverse Phase Liquid Chromatography coupled to MS (RP-LC-MS/MS) in an Agilent 1100 system coupled to a LTQ-Velos mass spectrometer (Thermo Scientific, Waltham, MA, USA). Peptides were separated using a 0.18 mm \times 150 mm Bio-Basic C18 RP column (Thermo Scientific, Waltham, MA, USA) at 1.8 μ L/min, using a 35 min gradient from 5–40% solvent A: 0.1% formic acid-solvent B: 0.1% formic acid, 80% acetonitrile. ESI ionization was performed using a microspray “metal needle kit” (Thermo Scientific, Waltham, MA, USA) interface. De Novo sequencing was carried out using PEAKS Studio 6 [48] (Bioinformatics Solutions, Waterloo, ON, Canada) at the Proteomic Service of Centro de Biología Molecular (CBMSO, Madrid, Spain).

For purification of the protein expressed in *P. pastoris*, transformants carrying the pIB4-derivative construction were cultivated in BMG, expression of proteins induced in BMM and heterologous activity evaluated in culture filtrates as referenced [34]. Empty pIB4 transformants were used as control. The extracellular fraction was concentrated and fractionated through 50,000 MWCO PES membranes and Amicon Ultra-15 ultracel-100K filters (if required). About 70–80% of the initial activity was recovered. PNGase F (Sigma-Aldrich, St. Louis, MO, USA), O-glycosidase+neuroaminidase and α -(1-2,3,6) mannosidase (both from NEB, Ipswich, MA, USA) treatments were performed according to manufacturer’s protocols.

4.3. Hydrolase Activity and Kinetic Analysis

Standard β -fructofuranosidase hydrolytic activity was evaluated using the dinitrosalicylic acid (DNS) method, as described [16]. Reactions (50 μ L) containing 5 μ L of enzymatic solutions (adequately diluted to fit the calibration curve) and 45 μ L of 2% sucrose in 50 mM sodium phosphate, pH 5.0, were incubated at 60 °C for 20 min, and then 50 μ L of DNS

was added. One unit of activity (U) was defined as catalyzing the formation of 1 μ mol of reducing sugar per minute under the described conditions. Estimation of the hydrolase activity at different pH (3.0–8.0) and temperature (40–80 °C) values was carried out under the aforementioned conditions using sucrose as substrate and sodium citrate (pH 3–4), sodium phosphate (pH 4–7), and Tris-HCl (pH 7–8), all 50 mM. 1-Kestose, nystose (both from TCI Europe N.V., Zwijndrecht, Belgium), raffinose (Sigma-Aldrich, St Louis, MO, USA), and inulin (Beneo, Barcelona, Spain) were tested, as referenced above.

The Michaelis–Menten kinetics constants were determined using sucrose (1.25–80 mM) or 1-kestose (5–100 mM). The plotting and analysis of curves were carried out using SigmaPlot V12.0, and the kinetic parameters calculated fitting the initial rate values to the Michaelis–Menten equation.

4.4. Transferase Activity, Fructooligosaccharides Production, and HPLC Analysis

The transferase activity analysis was performed in 600 g/L sucrose and 100 mM sodium acetate pH 5.5 containing 5 U/mL of enzymatic activity. Reactions were incubated at 60 °C in orbital shaker (Vortemp 56, Labnet International, Woodbridge, NJ, USA) at 600 rpm. Aliquots of 50 μ L were withdrawn at different times, incubated for 8 min at 100 °C, diluted 30 times in water, and filtered through nylon membranes of 0.45 μ m (Scharlab, Barcelona, Spain). Samples were analyzed by HPLC with a quaternary pump (Delta 600, Waters, Milford, CT, USA) coupled to a Liquid Purple amino column (4.6 \times 250 mm, from Análisis Vínicos, Tomelloso, Spain) and a precolumn-NH₂ (Phenomenex, Torrance, CA, USA). Detection was performed using an evaporative light scattering detector (ELSD; mod. 1000, Polymer Laboratories Ltd., Church Stretton, UK) equilibrated at 90 °C along with an automatic injector (mod. 717 Plus, Waters, Milford, CT, USA). An acetonitrile/water mixture, degassed with an in-line vacuum generator (ser. 200, Perkin-Elmer, Eden Prairie, MN, USA), was used as mobile phase at 1.0 mL/min during 45 min (first 10 min acetonitrile:water 85:15, changing to 75:25 over 2 min, and this proportion maintained until the end of the analysis). Temperature was 28 °C and volume injection 10 μ L. Data were analyzed using the Empower software (v.1.0; Waters). Compounds were quantified on the base of peak areas using the most closely related standard: glucose, fructose, sucrose, 1-kestose, nystose, neokestose, and neonystose, the last two produced from sucrose using β -fructofuranosidase from *X. dendrorhous* [34] and blastose and 6-kestose using the *Sch. occidentalis* enzyme [21,45].

Transfructosylation of potential acceptors by RdINV was assessed using 1 mL reactions containing 100 g/L acceptors and 100 g/L sucrose in 100 mM sodium acetate pH 5.5 for up to 180 min. Monosaccharides (fructose, glucose, galactose, xylose, L-arabinose, mannose), disaccharides (trehalose, isomaltulose, lactose, lactulose, leucrose, maltose, melibiose), and alditols (erythritol, galactitol, sorbitol, mannitol, ribitol, xylitol), all from Sigma-AldrichCorp. (St. Louis, MO, USA), were used. Negative controls included reactions without enzyme, sucrose, or alternative acceptors. Conditions and sample preparation were carried out as mentioned above. For HPLC-analysis of monosaccharides and sugar alcohols, a gradient phase was used with 80:20 acetonitrile:water for 18 min, followed by an increase of the water proportion to 30 for 30 min, and then return to the initial composition mixture (total analysis time: 35 min). For disaccharides, 80:20 acetonitrile:water was employed for 50 min.

4.5. DNA Techniques and Cloning of the *R. dairenensis* β -Fructofuranosidase

To characterize the gene responsible for the β -fructofuranosidase activity, total *R. dairenensis* DNA was obtained from a 16-h grown culture, as referenced [35], and used as template in PCR reactions. Initially, a 1268-bp fragment was obtained using the expand long template PCR System (Roche) with primers 1DE (+), 4RE (-), and 2RE (-) (Table S2), directed against part of the three tryptic peptides predicted from MS analysis of the RdINV protein (Table S1). Standard inverse PCR [35] was used to analyze the flanking region of the sequence characterized above. Briefly, genomic DNA was digested with *Cla*I or *Eco*RV.

Linear DNA (3 ng/μL) was circularized using T4 DNA ligase and used as a template with primers EC1D(+)+EC2R(-) and EC3D(+)+EC3R(-) (Table S2). PCR conditions were: 95 °C for 2 min, three cycles of 94 °C for 10 s, 55–60 °C for 30 s, and 68 °C for 2 min; then 35 cycles of 94 °C for 10 s, 55–60 °C for 30 s, and 68 °C for 1 min, increasing 5 s per cycle, and 7 min at 68 °C. PCR products were inserted into plasmid pST-Blue1 (Novagen, Darmstadt, Germany) and sequenced (Parque Científico-Madrid, Spain). A fragment of 2559-bp was obtained containing the potential RdINV gene of 2297-bp. The gene was amplified using primers EC8D(+)+EC8R(-), including *Kpn*I and *Spe*I restriction sites, respectively (Table S2), and inserted in plasmid pIB4, as referenced [34].

To eliminate the two potential introns identified in gene *RdINV* using NetAspGene 1.0 [49], a restriction-free cloning strategy based on two PCR reactions [50] and Phusion High Fidelity polymerase (NEB, Ipswich, MA, USA) were used. First, PCR was performed using construction RdINV-pIB4 as a template and RFint1F(+)+RFint2R(-) primers (Table S2) to amplify the exon 2 (858-bp) with flanking fragments of exon 1 and exon 3. PCR conditions were: 98 °C for 30 s, 10 cycles of 98 °C for 10 s, 55 °C for 30 s, and 72 °C for 30 s, then 25 cycles of 98 °C for 10 s and 72 °C for 1 min, and a final extension at 72 °C for 4 min. The fragment amplified and construction RdINV-pIB4 were used in the second PCR as megaprimer and template (in 50:1 molar ratio), respectively. PCR conditions were: 98 °C for 30 s, 35 cycles of 98 °C for 20 s, 55 °C for 35 s, and 72 °C for 5 min, then a final extension at 72 °C for 7 min. PCR mixture was digested with *Dpn*I and used to transform *E. coli*. The generated constructions RdINV- and cRdINV-pIB4 (including gene *RdINV* with or without introns respectively) were verified by sequencing and then linearized with *Stu*I for *P. pastoris* transformation.

4.6. Protein Sequence Analysis

The amino acid sequence deduced from gene *RdINV* was analyzed by NCBI pBLAST. Multiple alignment was arranged with T-coffee, and potential signal peptides were predicted with SignalP 4.1. Theoretical molecular weight and isoelectric point were calculated with ProtParam on ExPASy. N- and O-glycosylation were predicted using NetNGlyc 1.0 and GPP, respectively, and structural alignments occurred utilizing ENDscript, MSAProbs, and DSSP programs. The RdINV structural model was obtained by Phyre2 [51].

4.7. Nucleotide Sequence Accession Number

The sequence encoding the β-fructofuranosidase from *R. dairenensis* has been assigned the GenBank accession n° MH779452.

Supplementary Materials: The following are available online at <https://www.mdpi.com/article/10.3390/catal11040476/s1>, Table S1: Sequences derived from mass; Table S2: Primers used in this study; Figure S1: Overall structure of β-fructofuranosidase RdINV; Figure S2: Representative HPLC chromatograms from transfructosylating reactions containing sucrose and the referenced acceptors.

Author Contributions: Conceptualization and experiment design, M.F.-L. and M.G.-P.; performing most of the experiments and sequence analysis, M.G.-P., Z.M., E.C.-R. and C.M.d.H.; writing—original draft preparation, M.F.-L., M.G.-P. and Z.M.; supervision and funding acquisition, M.F.-L. All authors have read and agreed to the published version of the manuscript.

Funding: This work was supported by Spanish Ministry of Economy and Competitiveness: BIO2016-76601-C3-2 and of Science and Innovation PID2019-105838RB-C32; Fundación Ramón Areces (XIX Call of Research Grants in Life and Material Sciences); and by institutional grant from Fundación Ramón Areces to the Centro de Biología Molecular Severo Ochoa. CBMSO Proteomics Facility belongs to ProteoRed PRB2-ISCIII and was supported by the grant PT13/0001. M.G.-P. was supported by the Spanish Ministry of Education's University Personnel Training Plan (FPU).

Acknowledgments: We thank Asunción Martín Redondo for the technical support and Tom Halmos for manuscript corrections.

Conflicts of Interest: The authors declare no conflict of interest.

References

- Gibson, G.R.; Hutkins, R.; Sanders, M.E.; Prescott, S.L.; Reimer, R.A.; Salminen, S.J.; Scott, K.; Stanton, C.; Swanson, K.S.; Cani, P.D.; et al. Expert consensus document: The International Scientific Association for Probiotics and Prebiotics (ISAPP) consensus statement on the definition and scope of prebiotics. *Nat. Rev. Gastroenterol. Hepatol.* **2017**, *14*, 491–502. [\[CrossRef\]](#)
- Swennen, K.; Courtin, C.M.; Delcour, J.A. Non-digestible oligosaccharides with prebiotic properties. *Crit. Rev. Food Sci. Nutr.* **2006**, *46*, 459–471. [\[CrossRef\]](#) [\[PubMed\]](#)
- Battson, M.L.; Lee, D.M.; Weir, T.L.; Gentile, C.L. The gut microbiota as a novel regulator of cardiovascular function and disease. *J. Nutr. Biochem.* **2018**, *56*, 1–15. [\[CrossRef\]](#) [\[PubMed\]](#)
- Whisner, C.M.; Castillo, L.F. Prebiotics, bone and mineral metabolism. *Calcif. Tissue Int.* **2018**, *102*, 443–479. [\[CrossRef\]](#)
- Schachter, J.; Martel, J.; Lin, C.S.; Chang, C.J.; Wu, T.R.; Lu, C.C.; Ko, Y.F.; Lai, H.C.; Ojcius, D.M.; Young, J.D. Effects of obesity on depression: A role for inflammation and the gut microbiota. *Brain Behav. Immun.* **2018**, *69*, 1–8. [\[CrossRef\]](#)
- Chen, D.; Yang, X.; Yang, J.; Lai, G.; Yong, T.; Tang, X.; Shuai, O.; Zhou, G.; Xie, Y.; Wu, Q. Prebiotic effect of Fructooligosaccharides from *Morinda officinalis* on Alzheimer's disease in rodent models by targeting the microbiota-gut-brain axis. *Front. Aging Neurosci.* **2017**, *9*. [\[CrossRef\]](#) [\[PubMed\]](#)
- Man, S.; Liu, T.; Yao, Y.; Lu, Y.; Ma, L.; Lu, F. Friend or foe? The roles of inulin-type fructans. *Carbohydr. Polym.* **2021**, *252*, 117155. [\[CrossRef\]](#) [\[PubMed\]](#)
- Sabater-Molina, M.; Larqué, E.; Torrella, F.; Zamora, S. Dietary fructooligosaccharides and potential benefits on health. *J. Physiol. Biochem.* **2009**, *65*, 315–328. [\[CrossRef\]](#)
- Kilian, S.; Kritzinger, S.; Rycroft, C.; Gibson, G.; du Preez, J. The effects of the novel bifidogenic trisaccharide, neokestose, on the human colonic microbiota. *World J. Microbiol. Biotechnol.* **2002**, *18*, 637–644. [\[CrossRef\]](#)
- Wu, J.S.; Chang, J.Y.; Chen, C.W.; Lin, M.T.; Sheu, D.C.; Lee, S.M. Neokestose suppresses the growth of human melanoma A2058 cells via inhibition of the nuclear factor- κ B signaling pathway. *Mol. Med. Rep.* **2017**, *16*, 295–300. [\[CrossRef\]](#) [\[PubMed\]](#)
- Lee, S.M.; Chang, J.Y.; Wu, J.S.; Sheu, D.C. Antineoplastic effect of a novel chemopreventive agent, neokestose, on the Caco-2 cell line via inhibition of expression of nuclear factor- κ B and cyclooxygenase-2. *Mol. Med. Rep.* **2015**, *12*, 1114–1118. [\[CrossRef\]](#)
- Ni, D.; Xu, W.; Zhu, Y.; Pang, X.; Lv, J.; Mu, W. Insight into the effects and biotechnological production of kestoses, the smallest fructooligosaccharides. *Crit. Rev. Biotechnol.* **2021**, *41*, 34–46. [\[CrossRef\]](#)
- Singh, S.P.; Jadaun, J.S.; Narnoliya, L.K.; Pandey, A. Prebiotic oligosaccharides: Special focus on fructooligosaccharides, its biosynthesis and bioactivity. *Appl. Biochem. Biotechnol.* **2017**, *183*, 613–635. [\[CrossRef\]](#)
- Flores-Maltos, D.A.; Mussatto, S.I.; Contreras-Esquivel, J.C.; Rodríguez-Herrera, R.; Teixeira, J.A.; Aguilar, C.N. Biotechnological production and application of fructooligosaccharides. *Crit. Rev. Biotechnol.* **2016**, *36*, 259–267. [\[CrossRef\]](#) [\[PubMed\]](#)
- Marín-Navarro, J.; Talens-Perales, D.; Polaina, J. One-pot production of fructooligosaccharides by a *Saccharomyces cerevisiae* strain expressing an engineered invertase. *Appl. Microbiol. Biotechnol.* **2015**, *99*, 2549–2555. [\[CrossRef\]](#) [\[PubMed\]](#)
- Álvaro-Benito, M.; de Abreu, M.; Fernández-Arrojo, L.; Plou, F.J.; Jiménez-Barbero, J.; Ballesteros, A.; Polaina, J.; Fernández-Lobato, M. Characterization of a β -fructofuranosidase from *Schwanniomyces occidentalis* with transfructosylating activity yielding the prebiotic 6-kestose. *J. Biotechnol.* **2007**, *132*, 75–81. [\[CrossRef\]](#) [\[PubMed\]](#)
- Linde, D.; Rodríguez-Colinas, B.; Estévez, M.; Poveda, A.; Plou, F.J.; Fernández Lobato, M. Analysis of neofructooligosaccharides production mediated by the extracellular β -fructofuranosidase from *Xanthophyllomyces dendrorhous*. *Bioresour. Technol.* **2012**, *109*, 123–130. [\[CrossRef\]](#)
- Ramírez-Escudero, M.; Gimeno-Pérez, M.; González, B.; Linde, D.; Merdzo, Z.; Fernández-Lobato, M.; Sanz-Aparicio, J. Structural analysis of β -fructofuranosidase from *Xanthophyllomyces dendrorhous* reveals unique features and the crucial role of N-glycosylation in oligomerization and activity. *J. Biol. Chem.* **2016**, *291*, 6843–6857. [\[CrossRef\]](#) [\[PubMed\]](#)
- Sainz-Polo, M.A.; Ramírez-Escudero, M.; Lafraya, A.; González, B.; Marín-Navarro, J.; Polaina, J.; Sanz-Aparicio, J. Three-dimensional structure of *Saccharomyces* invertase: Role of a non-catalytic domain in oligomerization and substrate specificity. *J. Biol. Chem.* **2013**, *288*, 9755–9766. [\[CrossRef\]](#)
- Álvaro-Benito, M.; Polo, A.; González, B.; Fernández-Lobato, M.; Sanz-Aparicio, J. Structural and kinetic analysis of *Schwanniomyces occidentalis* invertase reveals a new oligomerization pattern and the role of its supplementary domain in substrate binding. *J. Biol. Chem.* **2010**, *285*, 13930–13941. [\[CrossRef\]](#)
- Álvaro-Benito, M.; Sainz-Polo, M.A.; González-Pérez, D.; González, B.; Plou, F.J.; Fernández-Lobato, M.; Sanz-Aparicio, J. Structural and kinetic insights reveal that the amino acid pair Gln-228/Asn-254 modulates the transfructosylating specificity of *Schwanniomyces occidentalis* β -fructofuranosidase, an enzyme that produces prebiotics. *J. Biol. Chem.* **2012**, *287*, 19674–19686. [\[CrossRef\]](#)
- Rubio, M.C.; Runco, R.; Navarro, A.R. Invertase from a strain of *Rhodotorula glutinis*. *Phytochemistry* **2002**, *61*, 605–609. [\[CrossRef\]](#)
- Hernalsteens, S.; Maugeri, F. Purification and characterisation of a fructosyltransferase from *Rhodotorula* sp. *Appl. Microbiol. Biotechnol.* **2008**, *79*, 589–596. [\[CrossRef\]](#)
- Canli Tasar, O. Enhanced β -fructofuranosidase biosynthesis by *Rhodotorula glutinis* using Taguchi robust design method. *Biocatal. Biotransform.* **2017**, *35*, 191–196. [\[CrossRef\]](#)
- Barbosa, P.M.G.; de Moraes, T.P.; de Andrade Silva, C.A.; da Silva Santos, F.R.; Garcia, N.F.L.; Fonseca, G.G.; Leite, R.S.R.; da Paz, M.F. Biochemical characterization and evaluation of invertases produced from *Saccharomyces cerevisiae* CAT-1 and *Rhodotorula mucilaginosa* for the production of fructooligosaccharides. *Prep. Biochem. Biotechnol.* **2018**, *48*, 506–513. [\[CrossRef\]](#)

26. Gutiérrez-Alonso, P.; Fernández-Arrojo, L.; Plou, F.J.; Fernández-Lobato, M. Biochemical characterization of a β -fructofuranosidase from *Rhodotorula dairenensis* with transfructosylating activity. *FEMS Yeast Res.* **2009**, *9*, 768–773. [\[CrossRef\]](#)
27. Lammens, W.; Le Roy, K.; Schroeven, L.; Van Laere, A.; Rabijns, A.; Van Den Ende, W. Structural insights into glycoside hydrolase family 32 and 68 enzymes: Functional implications. *J. Exp. Bot.* **2009**, *60*, 727–740. [\[CrossRef\]](#) [\[PubMed\]](#)
28. Pons, T.; Naumoff, D.G.; Martínez-Fleites, C.; Hernández, L. Three acidic residues are at the active site of a β -propeller architecture in Glycoside Hydrolase families 32, 43, 62, and 68. *Proteins Struct. Funct. Genet.* **2004**, *54*, 424–432. [\[CrossRef\]](#) [\[PubMed\]](#)
29. Trollope, K.M.; van Wyk, N.; Kotjomela, M.A.; Volschenk, H. Sequence and structure-based prediction of fructosyltransferase activity for functional sub-classification of fungal GH32 enzymes. *FEBS J.* **2015**, *282*, 1–15. [\[CrossRef\]](#)
30. Goordial, J.; Raymond-Bouchard, I.; Riley, R.; Ronholm, J.; Shapiro, N.; Woyke, T.; LaButti, K.M.; Tice, H.; Amirebrahimi, M.; Grigoriev, I.V.; et al. Improved high-quality draft genome sequence of the eurypsychrophile *Rhodotorula* sp. JG1b, isolated from permafrost in the hyperarid upper-elevation McMurdo Dry Valleys, Antarctica. *Genome Announc.* **2016**, *4*, 69–85. [\[CrossRef\]](#) [\[PubMed\]](#)
31. Paul, D.; Magbanua, Z.; Arick, M.; French, T.; Bridges, S.M.; Burgess, S.C.; Lawrence, M.L. Genome Sequence of the oleaginous yeast *Rhodotorula glutinis* ATCC 204091. *Genome Announc.* **2014**, *2*, 46–60. [\[CrossRef\]](#)
32. Zhu, Z.; Zhang, S.; Liu, H.; Shen, H.; Lin, X.; Yang, F.; Zhou, Y.J.; Jin, G.; Ye, M.; Zou, H.; et al. A multi-omic map of the lipid-producing yeast *Rhodospiridium toruloides*. *Nat. Commun.* **2012**, *3*, 1–12. [\[CrossRef\]](#)
33. Nagem, R.A.P.; Rojas, A.L.; Golubev, A.M.; Korneeva, O.S.; Eneyskaya, E.V.; Kulminkaya, A.A.; Neustroev, K.N.; Polikarpov, I. Crystal structure of exo-inulinase from *Aspergillus awamori*: The enzyme fold and structural determinants of substrate recognition. *J. Mol. Biol.* **2004**, *344*, 471–480. [\[CrossRef\]](#) [\[PubMed\]](#)
34. Gimeno-Pérez, M.; Linde, D.; Fernández-Arrojo, L.; Plou, F.J.; Fernández-Lobato, M. Heterologous overproduction of β -fructofuranosidase from yeast *Xanthophyllomyces dendrorhous*, an enzyme producing prebiotic sugars. *Appl. Microbiol. Biotechnol.* **2015**, *99*, 3459–3467. [\[CrossRef\]](#)
35. Linde, D.; Macias, I.; Fernández-Arrojo, L.; Plou, F.J.; Jiménez, A.; Fernández-Lobato, M. Molecular and biochemical characterization of a β -fructofuranosidase from *Xanthophyllomyces dendrorhous*. *Appl. Environ. Microbiol.* **2009**, *75*, 1065–1073. [\[CrossRef\]](#)
36. Nagaya, M.; Kimura, M.; Gozu, Y.; Sato, S.; Hirano, K.; Tochio, T.; Nishikawa, A.; Tono-zuka, T. Crystal structure of a β -fructofuranosidase with high transfructosylation activity from *Aspergillus kawachii*. *Biosci. Biotechnol. Biochem.* **2017**, *81*, 1786–1795. [\[CrossRef\]](#) [\[PubMed\]](#)
37. Henriksson, H.; Denman, S.E.; Campuzano, I.D.G.; Ademark, P.; Master, E.R.; Teeri, T.T.; Brumer, H. N-linked glycosylation of native and recombinant cauliflower xyloglucan endotransglycosylase 16A. *Biochem. J.* **2003**, *375*, 61–73. [\[CrossRef\]](#)
38. Han, M.; Wang, X.; Ding, H.; Jin, M.; Yu, L.; Wang, J.; Yu, X. The role of N-glycosylation sites in the activity, stability, and expression of the recombinant elastase expressed by *Pichia pastoris*. *Enzyme Microb. Technol.* **2014**, *54*, 32–37. [\[CrossRef\]](#) [\[PubMed\]](#)
39. Han, Y.; Wang, J.; Li, Y.; Wang, X.; Li, Q. Heterologous expression of *Hordeum vulgare* protein Z4 in *Pichia pastoris* shows increased structural stability. *Process Biochem.* **2016**, *51*, 828–837. [\[CrossRef\]](#)
40. Zambelli, P.; Fernandez-Arrojo, L.; Romano, D.; Santos-Moriano, P.; Gimeno-Perez, M.; Poveda, A.; Gandolfi, R.; Fernández-Lobato, M.; Molinari, F.; Plou, F.J. Production of fructooligosaccharides by mycelium-bound transfructosylation activity present in *Cladosporium cladosporioides* and *Penicillium sizovae*. *Process Biochem.* **2014**, *49*, 2174–2180. [\[CrossRef\]](#)
41. Santos-Moriano, P.; Fernandez-Arrojo, L.; Poveda, A.; Jimenez-Barbero, J.; Ballesteros, A.O.; Plou, F.J. Levan versus fructooligosaccharide synthesis using the levansucrase from *Zymomonas mobilis*: Effect of reaction conditions. *J. Mol. Catal. B Enzym.* **2015**, *119*, 18–25. [\[CrossRef\]](#)
42. Rodrigo-Frutos, D.; Piedrabuena, D.; Sanz-Aparicio, J.; Fernández-Lobato, M. Yeast cultures expressing the Ffase from *Schwanniomyces occidentalis*, a simple system to produce the potential prebiotic sugar 6-kestose. *Appl. Microbiol. Biotechnol.* **2019**, *103*, 279–289. [\[CrossRef\]](#) [\[PubMed\]](#)
43. Cervantes, F.V.; Neifar, S.; Merdzo, Z.; Viña-Gonzalez, J.; Fernandez-Arrojo, L.; Ballesteros, A.O.; Fernandez-Lobato, M.; Bejar, S.; Plou, F.J. A three-step process for the bioconversion of whey permeate into a glucose D-free tagatose syrup. *Catalysts* **2020**, *10*, 647. [\[CrossRef\]](#)
44. Gimeno-Pérez, M.; Santos-Moriano, P.; Fernandez-Arrojo, L.; Poveda, A.; Jimenez-Barbero, J.; Ballesteros, A.O.; Fernandez-Lobato, M.; Plou, F.J. Regioselective synthesis of neo-erlose by the β -fructofuranosidase from *Xanthophyllomyces dendrorhous*. *Process Biochem.* **2014**, *49*, 423–429. [\[CrossRef\]](#)
45. Piedrabuena, D.; Míguez, N.; Poveda, A.; Plou, F.J.; Fernández-Lobato, M. Exploring the transferase activity of Ffase from *Schwanniomyces occidentalis*, a β -fructofuranosidase showing high fructosyl-acceptor promiscuity. *Appl. Microbiol. Biotechnol.* **2016**, *100*, 8769–8778. [\[CrossRef\]](#) [\[PubMed\]](#)
46. Ruiz-Ojeda, F.J.; Plaza-Díaz, J.; Sáez-Lara, M.J.; Gil, A. Effects of sweeteners on the gut microbiota: A review of experimental studies and clinical trials. *Adv. Nutr.* **2019**, *10*, S31–S48. [\[CrossRef\]](#)
47. Lenhart, A.; Chey, W.D. A systematic review of the effects of polyols on gastrointestinal health and irritable bowel syndrome. *Adv. Nutr.* **2017**, *8*, 587–596. [\[CrossRef\]](#)
48. Zhang, J.; Xin, L.; Shan, B.; Chen, W.; Xie, M.; Yuen, D.; Zhang, W.; Zhang, Z.; Lajoie, G.A.; Ma, B. PEAKS DB: De novo sequencing assisted database search for sensitive and accurate peptide identification. *Mol. Cell. Proteom.* **2012**, *11*. [\[CrossRef\]](#)

-
49. Wang, K.; Ussery, D.W.; Brunak, S. Analysis and prediction of gene splice sites in four *Aspergillus* genomes. *Fungal Genet. Biol.* **2009**, *46* (Suppl. 1), S14–S18. [[CrossRef](#)]
 50. Van Den Ent, F.; Löwe, J. RF cloning: A restriction-free method for inserting target genes into plasmids. *J. Biochem. Biophys. Methods* **2006**, *67*, 67–74. [[CrossRef](#)]
 51. Kelley, L.A.; Sternberg, M.J.E. Protein structure prediction on the Web: A case study using the Phyre server. *Nat. Protoc.* **2009**, *4*, 363–371. [[CrossRef](#)] [[PubMed](#)]